

Energy Density Distribution in Bridged Cobalt Complexes

Markus Finger and Joachim Reinhold*

Wilhelm-Ostwald-Institut für Physikalische und Theoretische Chemie, Universität Leipzig,
D-04103 Leipzig, Germany

Received August 28, 2003

In the theory of atoms in molecules (AIM), the charge density is usually a suitable tool for bonding analyses. However, problems arise in some cases. So, no direct Co–Co bond is found in $\text{Co}_2(\text{CO})_8$. It is shown that the energy density gives deeper insight into the bonding properties. This is demonstrated for $\text{Co}_2(\text{CO})_8$, $\text{Co}_4(\text{CO})_{12}$, and $\text{Co}_2(\text{CO})_6(\text{InMe})_2$. The strategy is not restricted to transition metal compounds; it should be useful to identify any weak bonding or antibonding interactions.

Bader's theory of atoms in molecules (AIM)¹ is nowadays widely accepted in population and bonding analyses. In this theory, a bond is generally indicated by the existence of a bond critical point (*bcp*) characterized by the minimum of the charge density ρ along the path of maximum charge density between two atoms. More specific information concerning the nature of the molecular interactions is provided by the Laplacian $\nabla^2\rho$ of the charge density, distinguishing between regions of charge accumulation and charge depletion. It has been shown by Cremer and Kraka that the energy density H , resulting as the sum of the kinetic energy density G and the potential energy density V , is even more sensitive for analyzing bonding effects.^{2,3} *Bcp*'s of negative energy density are assigned to be bonding.

Despite the capacity of the method, only a few AIM analyses for complexes featuring bonds between transition metal centers have been published. Among the considered systems, $\text{Co}_2(\text{CO})_8$ received special attention. For this compound, the 18-electron rule predicts a direct Co–Co bond. However, this so-called bent bond is still a matter of controversy. Neither the molecular orbitals picture gives a clear answer, nor deformation density maps.^{4,5} An AIM analysis could open a new view. But, as already pointed out by Low

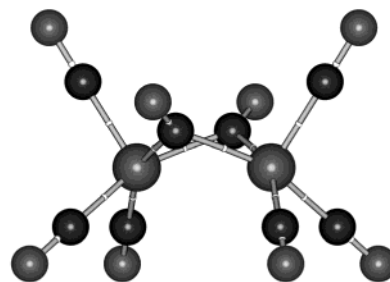


Figure 1. Structure of $\text{Co}_2(\text{CO})_8$ (*bcp*'s are indicated by white dots).

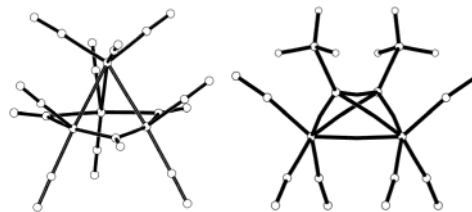


Figure 2. Structures of $\text{Co}_4(\text{CO})_{12}$ and $\text{Co}_2(\text{CO})_6(\text{InMe})_2$.

*et al.*⁵ and Macchi *et al.*,⁶ no Co–Co *bcp* exists (see Figure 1). Correspondingly, for the related $\text{Co}_4(\text{CO})_{12}$ system (see Figure 2), Macchi *et al.* obtained Co–Co *bcp*'s only between the unbridged, but not between the bridged Co centers.⁷

Otherwise, *bcp*'s between bridged metal centers were found in the case of various bridging ligands except CO.⁸ As expected, metal–metal bonds appear to be rather weak in comparison to metal–ligand bonds (see Table 1). The question arises, whether the charge density characteristics related to Co–Co bent bonds in $\text{Co}_2(\text{CO})_8$ and $\text{Co}_4(\text{CO})_{12}$ might be overwhelmed by the charge density related to the much stronger Co–CO bonds. Macchi *et al.* denied this conclusion for $\text{Co}_4(\text{CO})_{12}$.⁷

To investigate the bent-bond problem in further detail, we have examined various charge and energy densities along lines crossing the respective bonding regions, i.e., the charge

* Author to whom correspondence should be addressed. E-mail: reinhold@quant1.chemie.uni-leipzig.de.

(1) Bader, R. F. W. *Atoms in Molecules*; Clarendon Press: Oxford, 1990.

(2) (a) Cremer, D.; Kraka, E. *Angew. Chem., Int. Ed. Engl.* **1984**, *23*, 627. (b) Cremer, D.; Kraka, E. *Croat. Chem. Acta* **1984**, *57*, 1259.

(3) In detail, the energy densities are as follows: kinetic energy density $G(\mathbf{r}) = \frac{1}{2}N/\nabla\Psi^*\nabla\Psi \, d\mathbf{r}'$, potential energy density $V(\mathbf{r}) = N/\Psi^*(-\mathbf{r}\nabla V_0)\Psi \, d\mathbf{r}'$, (total) energy density $H(\mathbf{r}) = G(\mathbf{r}) + V(\mathbf{r})$, where \mathbf{r}' indicates integration over the coordinates of all electrons but one. V_0 is the potential operator.^{1,2} The energy densities are connected with the Laplacian of the charge density by Bader's formula $2G(\mathbf{r}) + V(\mathbf{r}) = \frac{1}{4}\nabla^2\rho(\mathbf{r}) = -L(\mathbf{r})$.¹

(4) Leung, P. C.; Coppens, P. *Acta Crystallogr.* **1983**, *B 39*, 535.

(5) Low, A. A.; Kunze, K. L.; MacDougall, P. J.; Hall, M. B. *Inorg. Chem.* **1991**, *30*, 1079.

(6) Macchi, P.; Sironi, A. *Coord. Chem. Rev.* **2003**, *238/239*, 363.

(7) Macchi, P.; Garlaschelli, L.; Martinengo, S.; Sironi, A. *J. Am. Chem. Soc.* **1999**, *121*, 10428.

(8) (a) Bianchi, R.; Gervasio, G.; Marabello, D. *Helv. Chim. Acta* **2001**, *84*, 722. (b) Bianchi, R.; Gervasio, G.; Marabello, D. *Acta Crystallogr.* **2001**, *B57*, 638. (c) Uhl, W.; Melle, S.; Frenking, G.; Hartmann, M. *Inorg. Chem.* **2001**, *40*, 750.

Table 1. Examples of *bcp* Characteristics of Metal–Metal Bonds in Binuclear Complexes (ρ and H in $\text{au}/\text{\AA}^{-3}$, $\nabla^2\rho$ in $\text{au}/\text{\AA}^{-5}$)^a

		d^b	ρ_c	$\nabla^2\rho_c$	H_c
Unbridged Metal–Metal Bonds					
$\text{Mn}_2(\text{CO})_{10}$	exptl ^c	290.4	0.190	0.815	−0.031
$\text{Co}_2(\text{CO})_6(\text{AsPh}_3)_2$	exptl ^d	264.3	0.204	1.344	−0.025
	calcd ^d	264.0	0.271	0.043	−0.090
$\text{Co}_4(\text{CO})_{11}(\text{PPh}_3)$	exptl ⁷	252.8	0.252	1.81	−0.039
$\text{Co}_4(\text{CO})_{12}$	calcd ⁷	252.0	0.355	−0.11	−0.152
$\text{Co}_2(\text{CO})_8$ (D_{3d})	calcd ⁶	274.6	0.227	0.06	−0.063
Bridged Metal–Metal Bonds					
$\text{Co}_2(\text{CO})_7(\text{C}_2\text{O}_4\text{H}_2)$	exptl ^{8a}	242.2	0.76	2.0	−0.46
$\text{Co}_2(\text{CO})_7(\text{C}_2\text{O}_4\text{H}_2)$	exptl ^{8b}	244.0	0.46	3.4	
$\text{Ni}_2\text{Cp}_2(\text{InCH}_3)_2$	calcd ^{8c}	249.1	0.282	0.809	−0.074
$\text{Ni}_2\text{Cp}_2(\text{GaCH}_3)_2$	calcd ^{8c}	244.9	0.300	1.118	−0.075
Co–CO (terminal)	calcd ^e		0.927	12.76	−0.34

^a For comparison, a metal–ligand bond in $\text{Co}_2(\text{CO})_8$ is included.

^b M–M bond length in pm. ^c Bianchi, R.; Gervasio, G.; Marabello, D. *Inorg. Chem.* **2000**, *39*, 2360. ^d Macchi, P.; Proserpio, M.; Sironi, A. *J. Am. Chem. Soc.* **1998**, *120*, 13429. ^e This work.

density ρ , the energy density L related to the Laplacian $\nabla^2\rho$ of the charge density, the kinetic energy density G , the potential energy density V , and the (total) energy density H .

DFT calculations in the idealized experimental structures^{4,7,10} applying the B3LYP¹¹ functionals were performed using the Gaussian98 program package.¹² For cobalt and indium a (14s,11p,6d,3f)/[8s,6p,4d,1f] and a (19s,15p,9d)/[8s,7p,5d], respectively, all-electron basis¹³ was used, whereas for the other atoms the standard 6-31G* basis sets¹⁴ were used throughout. The bonding analyses were undertaken with EXTREME contained in the AIMPAC package¹⁵ of Bader.

In Figure 3, the results for $\text{Co}_2(\text{CO})_8$ are presented. The densities along the 2-fold symmetry axis are displayed in dependence on the distance from the Co–Co vector. The maximum of the charge density ρ , which is a minimum in the perpendicular plane, represents a ring critical point. The minimum of L indicates repulsive interactions between the cobalt–ligand bonds. The energy densities G and V also show extrema in this area. The energy density H , however,

(9) $L = -1/4\nabla^2\rho$ is used instead of the Laplacian to allow the simultaneous presentation of all densities in one graph.

(10) Uhl, W.; Keimling, S. U.; Hiller, W.; Neumayer, M. *Chem. Ber.* **1996**, *129*, 397.

(11) (a) Becke, A. D. *J. Chem. Phys.* **1993**, *98*, 5648. (b) Lee, C.; Yang, W.; Parr, R. G. *Phys. Rev.* **1988**, *B 37*, 785.

(12) Frisch, M. J.; Trucks, G. W.; Schlegel, H. B.; Scuseria, G. E.; Robb, M. A.; Cheeseman, J. R.; Zakrzewski, V. G.; Montgomery, J. A., Jr.; Stratmann, R. E.; Burant, J. C.; Dapprich, S.; Millam, J. M.; Daniels, A. D.; Kudin, K. N.; Strain, M. C.; Farkas, O.; Tomasi, J.; Barone, V.; Cossi, M.; Cammi, R.; Mennucci, B.; Pomelli, C.; Adamo, C.; Clifford, S.; Ochterski, J.; Petersson, G. A.; Ayala, P. Y.; Cui, Q.; Morokuma, K.; Malick, D. K.; Rabuck, A. D.; Raghavachari, K.; Foresman, J. B.; Cioslowski, J.; Ortiz, J. V.; Stefanov, B. B.; Liu, G.; Liashenko, A.; Piskorz, P.; Komaromi, I.; Gomperts, R.; Martin, R. L.; Fox, D. J.; Keith, T.; Al-Laham, M. A.; Peng, C. Y.; Nanayakkara, A.; Gonzalez, C.; Challacombe, M.; Gill, P. M. W.; Johnson, B.; Chen, W.; Wong, M. W.; Andres, J. L.; Gonzalez, C.; Head-Gordon, M.; Replogle, E. S.; Pople, J. A. *Gaussian 98*, revision A.11.3; Gaussian Inc.: Pittsburgh, PA, 1998.

(13) (a) Wachters, A. J. H. *J. Chem. Phys.* **1970**, *52*, 1033. (b) Bauschlicher, C. W., Jr.; Langhoff, S. R.; Barnes, L. A. *J. Chem. Phys.* **1989**, *91*, 2399. (c) Ahlrichs, R.; May, K. *Phys. Chem. Chem. Phys.* **2000**, *2*, 943.

(14) Hehre, W. J.; Radom, L.; Schleyer, P. v. R.; Pople, J. *Ab-initio Molecular Orbital Theory*; Wiley: New York, 1986.

(15) Biegler-König, F. W.; Bader, R. F. W.; Tang, T.-H. *J. Comput. Chem.* **1982**, *3*, 317.

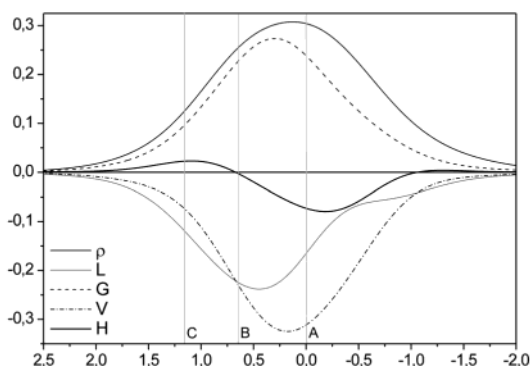


Figure 3. Charge density ρ and energy densities (in $\text{au}/\text{\AA}^{-3}$) along the 2-fold axis in $\text{Co}_2(\text{CO})_8$. L is equivalent to the negative of the Laplacian, and G and V are the kinetic and potential energy densities, respectively, whereas H sums up both contributions. Lines A, B, and C indicate the positions of the Co–Co, C–C, and O–O connecting vectors, respectively.

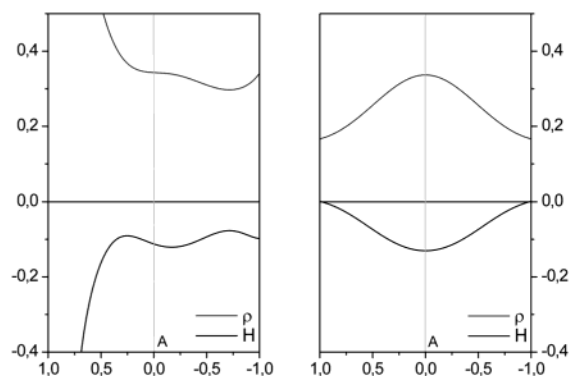


Figure 4. Charge density ρ and energy density H (in $\text{au}/\text{\AA}^{-3}$) in $\text{Co}_4(\text{CO})_{12}$ along a line perpendicular to the Co–Co bonds. For the bridged bond (left), this line points from the bridging CO “inside”; for the unbridged bond (right), it is normal to the symmetry plane. Line A indicates the position of the Co–Co vector.

turns out to be more sensitive than its individual contributions. It shows a distinct minimum in the bent-bond region and a maximum between the bridging CO's.

The formation of a chemical bond is connected with a decrease of the total energy of the system. The larger this energy decrease, the more stable is the resulting bond. By examining the energy density H , the local contributions to the total molecular electronic energy can be discussed. Attractive interactions are represented by negative values of H , contributing to the decrease of the total molecular energy. Accordingly, we interpret the obtained minimum of H , which is also a minimum in the perpendicular plane, as a direct Co–Co bonding interaction, not only supporting the prediction of the 18-electron rule but also showing a slight but distinct bending. Contrary, repulsive interactions are connected with positive values of H having an increasing effect on the total molecular energy. Consequently, the maximum of H clearly indicates repulsive interactions between the two bridging CO's. This agrees with results recently obtained in a different way for derivatives of $\text{Fe}_2(\text{CO})_9$.¹⁶

The essential results for $\text{Co}_4(\text{CO})_{12}$ are presented in Figure 4. Again, a slightly bent direct bonding interaction between

(16) (a) Barthel, A.; Mealli, C.; Uhl, W.; Reinhold, J. *Organometallics* **2001**, *20*, 786. (b) Reinhold, J.; Barthel, A.; Mealli, C. *Coord. Chem. Rev.* **2003**, *238/239*, 333.

COMMUNICATION

the bridged Co centers is indicated by the minimum of H . For the unbridged bonds, the minimum of H corresponds to the *bcp* position situated between the two Co centers (line A). Remarkably, for both cases, comparable charge and energy characteristics result.¹⁷

We extended the investigations to $\text{Co}_2(\text{CO})_6(\mu\text{-InMe})_2$, a derivative of $\text{Co}_2(\text{CO})_8$, in which the bridging CO's are substituted by indyl ligands. Now, a *bcp* between the two Co centers results. This is somewhat surprising, because the Co–Co distance is around 30 pm longer than in the parent compound, for which no *bcp* exists. The energy density H , however, shows a similar minimum for both systems (compare Figure 5 with Figure 3). The only difference is that the direct Co–Co bond is not bent. By using a sufficiently extended (*triple- ζ*) basis set for In, an additional weak bonding interaction between the two In centers is found, indicated by a *bcp* and a flat minimum of H . Thus, the bridging moiety in $\text{Co}_2(\text{CO})_6(\mu\text{-InR})_2$ can be considered as a Co_2In_2 cluster unit, which has been assumed by Uhl *et al.*¹⁰ for $\text{R} = \text{C}(\text{SiMe}_3)_3$.

It has turned out that, in many cases, the investigation of the topology of the *charge* density is an appropriate way for

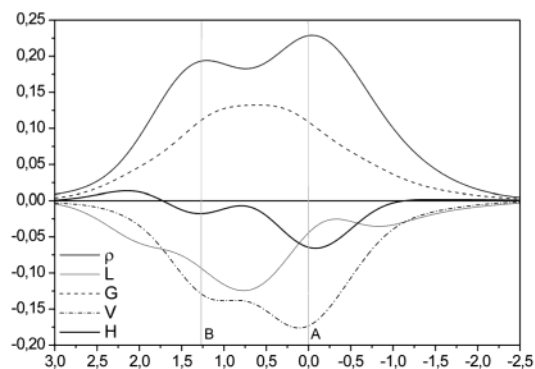


Figure 5. Charge and energy densities (in $\text{au}/\text{\AA}^{-3}$) along the 2-fold axis in $\text{Co}_2(\text{CO})_6(\mu\text{-InMe})_2$. Lines A and B indicate the positions of the Co–Co and In–In connecting vectors, respectively.

bonding analyses. However, weak bonding interactions as metal–metal bonds might be overwhelmed. In such cases, the *energy* density can be a valuable tool for a careful and sensitive bonding analysis. The strategy is not restricted to transition metal compounds; it should be useful to identify any weak bonding or antibonding interactions.

Acknowledgment. We thank the Fonds der Chemischen Industrie for financial support.

IC035011I

(17) The differences in the charge densities obtained by Macchi *et al.*⁷ seem to be caused by using Hartree–Fock densities.